

A quadratic convex framework with bigger freedom for the stability analysis of a cyber-physical microgrid system

Jing HE^{1,2}, Yan LIANG^{1,2}, Xiaohui HAO^{1,2}, Feisheng YANG^{1,2*} & Quan PAN^{1,2}

¹*School of Automation, Northwestern Polytechnical University, Xi'an 710072, China;*

²*Key Laboratory of Information Fusion Technology, Ministry of Education, Xi'an 710072, China*

Received 8 May 2021/Revised 20 October 2021/Accepted 11 February 2022/Published online 11 January 2023

Abstract Information exchange between a microgrid central controller and local controllers is supported by low-bandwidth communication channels, leading to an inevitable delay with time-varying characteristics that adversely affect the microgrid dynamics and even cause instability. This study addresses the problem of stability analysis for a load frequency control (LFC) microgrid system with the interval time-varying delay. First, a modeling approach is proposed for the cyber-physical microgrid, in which the physical interconnection between the cyber-physical components is established. Given that a quadratic function is often introduced in stability analysis and the negative determination is crucial to reducing the conservatism, a novel quadratic convex framework with adjustable free parameters that relaxes the quadratic function negative-determination conditions is developed. Next, the delay-dependent stability criterion of the cyber-physical LFC microgrid is obtained on the basis of augmented Lyapunov-Krasovskii functional and Bessel-Legendre inequality together with mixed convex combination techniques. This reduces the conservatism without requiring extra decision variables. Finally, two types of case studies demonstrate the merits of the proposed scheme.

Keywords cyber-physical microgrid, load frequency control, quadratic convex framework, stability analysis

Citation He J, Liang Y, Hao X H, et al. A quadratic convex framework with bigger freedom for the stability analysis of a cyber-physical microgrid system. *Sci China Inf Sci*, 2023, 66(2): 122202, <https://doi.org/10.1007/s11432-021-3433-8>

1 Introduction

A microgrid is a group of distributed energy resources, including renewable energy sources (RESs) and energy storage systems, together with plus loads that operate locally as a single controllable entity [1–3]. A microgrid contains different types of microsources, such as the gas-based microturbine, wind turbine, solar photovoltaic (PV) panel, fuel cell (FC), and electrolyzer system (ES). The load generally consists of a residential or small-scale industrial load. With the growing deployment of RESs, the stability analysis and control of microgrid systems have become increasingly active [4]. Frequency regulation is a major concern, and the load frequency control (LFC) strategy is effectively used to guarantee a stable operation of microgrid systems with an expected frequency [5].

To achieve the ultimate goal of stable operation with a desirable frequency, a hierarchical control structure that includes a micro-grid central controller (MGCC) and local controllers (LCs) is used [6]. Information exchange in such a control structure is performed through an open communication network [7–12]. Such a cyberinfrastructure brings out a considerable time delay in transmission that adversely affects the microgrid dynamics and even causes instability [13–16]. Most of the existing studies on the implementation of a conventional LFC strategy for microgrids generally ignore the delay mainly because the characteristic equation of the microgrid system with time delay is exponentially transcendent with infinite-dimensional characteristics, and difficult to analyze.

At present, few studies have considered the time delay and computed the stability delay margin. They are classified into two types. One type treats the time delay in the microgrid LFC system as a constant

* Corresponding author (email: yangfeisheng@nwpu.edu.cn)

value, and analyzes the system performance based on the frequency domain analytical method [17]. Such an exact approach can be used to obtain the accurate value of the delay margin. However, the delay is actually time-varying within an interval for a given transmission control protocol/Internet protocol (TCP/IP)-based communication channel. The other type focuses on proposing a stability condition of the cyber-physical LFC microgrid with time-varying delay using Lyapunov-Krasovskii functional (LKF) with the following developments and shortcomings [18–21].

- In terms of the problem considered, most results depend on the known information regarding the delay derivative, leading to several limitations. When it involves unknown bounds of the delay derivative or fast-varying delay in the microgrid, the abovementioned results will no longer be applicable. In addition, all of the abovementioned studies assumed that the lower bound of delay would be 0. In fact, such an assumption is very peculiar in an actual microgrid.

- In terms of specific implementation technology, the key mainly lies in the development of different LKFs (e.g., augmented LKF [22], multiintegral-based LKF [23], delay-product-type LKF [24,25], matrix-refined-function-based LKF [26]) and the inequality techniques for estimating the LKF derivatives (see Jensen inequality [27], Wirtinger-based inequality [28], auxiliary-based inequality [29], free-weighting-matrix approach [30], and Bessel-Legendre (B-L)-based inequality [31]). However, for the stability of a cyber-physical LFC time-delay microgrid system, there is still no perfect way to deal with the time-varying delay or the obtained stability criteria are more conservative. These two aspects motivate the current research.

Among the abovementioned approaches, the high-order B-L inequality together with appropriate LKFs has the potential to reduce conservatism. Sometimes for the constructed functionals to contain more information regarding the time delay and the coupling matrix, some quadratic terms of the delay are introduced, which may also appear in the LKF derivatives. The following main technical difficulties arise: (1) how to determine the negativity conditions of the quadratic function for obtaining the tractable linear matrix inequality (LMI)-based stability criteria, and (2) if it is possible to relax the quadratic function negative-determination conditions such that they are conducive to obtaining the stability criteria with less conservatism for a cyber-physical LFC microgrid system.

In response to the abovementioned motivations and difficulties, the main contributions of this study are highlighted as follows. (1) The stability analysis of a cyber-physical LFC microgrid with interval time-varying delay, i.e., $d(t) \in [d_1, d_2]$, where $d_1 \geq 0$ is the lower bound of the communication delay and d_2 is the admitted maximum delay bound (AMDB) without losing asymptotic stability, is presented. Notably, no knowledge of the $\dot{d}(t)$ boundary is acquired here. (2) A parameter-adjustable quadratic convex framework is developed to relax the quadratic function negative-determination conditions. (3) Using the augmented LKF and the second-order B-L inequality together with mixed convex combination techniques, the delay-dependent stability criteria of the cyber-physical LFC microgrid are obtained, which reduces the conservatism without requiring additional decision variables. Finally, simulations are conducted on a well-known numerical example and the LFC microgrid example. The relationship between the AMDB and MGCC gain is explored, which guides the selection of the microgrid controller. In addition, the superiority of this article's approach is demonstrated by comparing it with the representative methods.

The remaining paper is organized as follows. The LFC microgrid model is proposed in Section 2, and the development of a novel quadratic convex framework is presented in Section 3. New stability analysis criteria are derived in Section 4, and simulation results are provided in Section 5. Finally, the conclusion is presented in Section 6.

Notations. \mathbb{R}^n denotes the n -dimensional Euclidean space and $\mathbb{R}^{m \times n}$, \mathbb{S}^n , and \mathbb{S}_+^n are the sets of $m \times n$ real matrices, $n \times n$ real symmetric matrices and $n \times n$ symmetric positive definite matrices, respectively. “T” and “ -1 ” represent the transpose and inverse of a matrix, respectively. “*” represents the term induced by symmetry in a symmetric matrix. $\text{col}\{\cdot\}$ denotes a block-column matrix. $\text{diag}\{\cdot\}$ denotes a block-diagonal matrix. I is an identity matrix, and $\text{sym}\{A\}$ stands for $A + A^T$.

2 Cyber-physical LFC microgrid model

A major challenge in the microgrid system is the integration of communication and control, which is usually called a cyber-physical energy system. The embedded network monitors and controls the physical process through the feedback loop and the physical process affects the calculation and vice versa. This

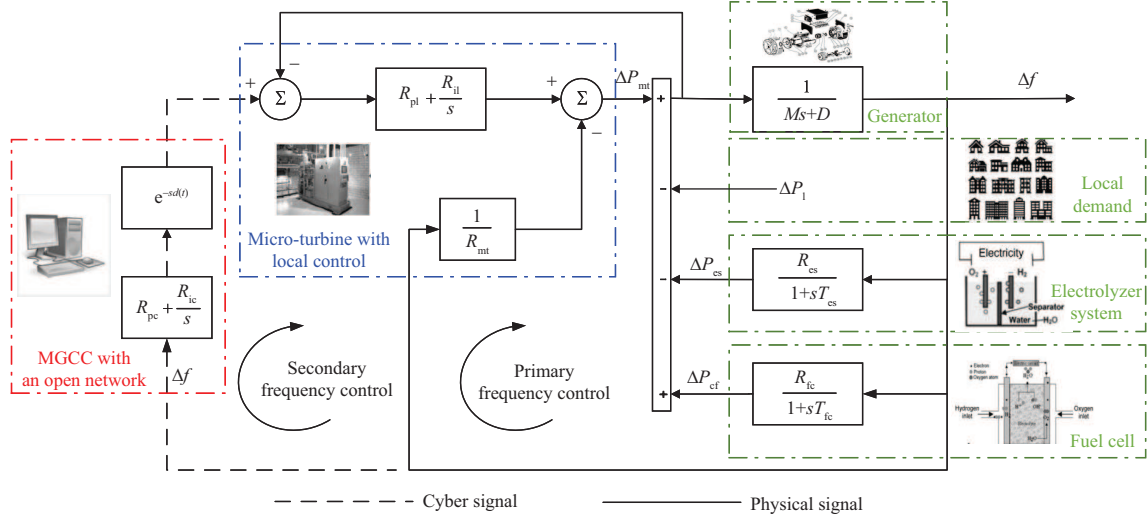

Figure 1 (Color online) The structure of the cyber-physical LFC microgrid model.

Table 1 Notations and descriptions

Notation	Description
Δf	Deviation of frequency
ΔP_{es}	Output of electrolyzer system
ΔP_{fc}	Output of fuel cell
ΔP_{mt}	Change in output power
ΔP_l	Disturbance of load
M	Moment of inertia of generator
D	Damping constant of generator
R_{es}	Gain of electrolyzer system
T_{es}	Time constant of electrolyzer system
R_{fc}	Gain of fuel cell
T_{fc}	Time constant of fuel cell
R_{mt}	Drop characteristics of the micro-turbine
R_{pl}	Proportional gain of local controller
R_{il}	Integral gain of local controller
R_{pc}	Proportional gain of central controller
R_{ic}	Integral gain of central controller

study proposes a cyber-physical system modeling approach for the microgrid. Figure 1 presents the block diagram and Table 1 gives the notations.

As shown in Figure 1, the dynamic model of cyber-physical microgrid system is described as follows:

$$R_{ic} \int \Delta f dt = R_{ic} \Delta f, \quad (1a)$$

$$\Delta \dot{P}_{fc} = -\frac{1}{T_{fc}} \Delta P_{fc} + \frac{R_{fc}}{T_{fc}} \Delta f, \quad (1b)$$

$$\Delta \dot{P}_{es} = -\frac{1}{T_{es}} \Delta P_{es} + \frac{R_{es}}{T_{es}} \Delta f, \quad (1c)$$

$$\Delta \dot{f} = \frac{1}{M} \Delta P_{mt} + \frac{1}{M} \Delta P_{fc} - \frac{1}{M} \Delta P_{es} - \frac{D}{M} \Delta f, \quad (1d)$$

$$\begin{aligned} \Delta \dot{P}_{mt} = & \frac{1}{1 + R_{pl}} \left\{ \left(-R_{il} - \frac{1}{MR_{mt}} \right) \Delta P_{mt} + \left(\frac{R_{pl}}{T_{fc}} - R_{il} - \frac{1}{MR_{mt}} \right) \Delta P_{fc} \right. \\ & + \left. \left(-\frac{R_{pl}}{T_{es}} + R_{il} + \frac{1}{MR_{mt}} \right) \Delta P_{es} + \left(-\frac{R_{pl}R_{fc}}{T_{fc}} + \frac{R_{pl}R_{es}}{T_{es}} + \frac{D}{MR_{mt}} \right) \Delta f \right. \\ & \left. - R_{il}R_{ic} \int \Delta f(t - d(t))dt - \frac{R_{pc}R_{pl}}{M} \Delta P_m(t - d(t)) \right\} \end{aligned}$$

$$\begin{aligned}
 & -\frac{R_{pc}R_{pl}}{M}\Delta P_{fc}(t-d(t)) + \frac{R_{pc}R_{pl}}{M}\Delta P_{es}(t-d(t)) \\
 & + \left(\frac{R_{pc}R_{pl}D}{M} - R_{pc}R_{il} - R_{ic}R_{pl} \right) \Delta f(t-d(t)) \Big\}. \tag{1e}
 \end{aligned}$$

Defining the system state vector as $x(t) = [R_{ic} \int \Delta f dt, \Delta P_{mt}, \Delta P_{fc}, \Delta P_{es}, \Delta f]^T$ and according to (1), the state-space model of the cyber-physical LFC microgrid is given below [18, 21]:

$$\begin{cases} \dot{x}(t) = Ax(t) + A_d x(t-d(t)) + F \Delta P'_1, \\ x(t) = \phi(t), \quad t \in [-d_2, 0], \end{cases} \tag{2}$$

where

$$\begin{aligned}
 A &= \begin{bmatrix} 0 & 0 & 0 & 0 & R_{ic} \\ 0 & a_{22} & a_{23} & a_{24} & a_{25} \\ 0 & 0 & -\frac{1}{T_{fc}} & 0 & \frac{R_{fc}}{T_{fc}} \\ 0 & 0 & 0 & -\frac{1}{T_{es}} & \frac{R_{es}}{T_{es}} \\ 0 & \frac{1}{M} & \frac{1}{M} & -\frac{1}{M} & -\frac{D}{M} \end{bmatrix}, \quad A_d = \begin{bmatrix} 0_{5 \times 1} & a_d & 0_{5 \times 1} & 0_{5 \times 1} & 0_{5 \times 1} \end{bmatrix}^T, \quad F = \begin{bmatrix} 0 & 0 \\ \frac{R_{pl}}{1+R_{pl}} & \frac{R_{il}}{1+R_{pl}} \\ 0 & 0 \\ 0 & 0 \\ 0 & -\frac{1}{M} \end{bmatrix}, \\
 \Delta P'_1 &= \begin{bmatrix} \Delta P_1 \\ \Delta P_1 \end{bmatrix}, \quad a_{22} = a \left(-R_{il} - \frac{1}{MR_{mt}} \right), \quad a = \frac{1}{1+R_{pl}}, \\
 a_{23} &= a \left(\frac{R_{pl}}{T_{fc}} - R_{il} - \frac{1}{MR_{mt}} \right), \quad a_{24} = a \left(-\frac{R_{pl}}{T_{es}} + R_{il} + \frac{1}{MR_{mt}} \right), \\
 a_{25} &= a \left(-\frac{R_{pl}R_{fc}}{T_{fc}} + \frac{R_{pl}R_{es}}{T_{es}} + \frac{D}{MR_{mt}} \right), \quad a_d = \begin{bmatrix} a_{d,21} & a_{d,22} & a_{d,23} & a_{d,24} & a_{d,25} \end{bmatrix}^T, \\
 a_{d,21} &= -aR_{il}, \quad a_{d,22} = a_{d,23} = -a_{d,24} = -a\frac{R_{pc}R_{pl}}{M}, \\
 a_{d,25} &= a \left(\frac{R_{pc}R_{pl}D}{M} - R_{pc}R_{il} - R_{ic}R_{pl} \right), \tag{3}
 \end{aligned}$$

and $\phi(t)$ denotes the initial condition. The time-varying delay $d(t)$ satisfies $0 \leq d_1 \leq d(t) \triangleq \tau \leq d_2$ with d_1, d_2 being constants and $d_{12} \triangleq d_2 - d_1$. According to [32, 33], external interference does not affect the internal stability. Therefore, $F \Delta P'_1$ can be ignored for the stability analysis of the cyber-physical LFC microgrid with time-varying delay.

Since the quadratic function is usually introduced in the stability analysis, and the determination of its negative definite condition is the key to reducing the conservatism, the next goal is to provide a novel quadratic convex framework for relaxing the quadratic function negative-determination condition. Furthermore, we will derive new stability criteria for the cyber-physical LFC microgrid system.

3 A quadratic convex framework with bigger freedom

The novel quadratic convex framework is developed to find negativity conditions of quadratic functions with bigger freedom. It is important to obtain less conservative results in sequel.

Lemma 1. For $a_2, a_1, a_0 \in \mathbb{R}$, $\alpha_{Mm} \in [0, 1]$, $m = 1, 2, \dots, M$, where M is a positive integer, a quadratic function $f(\tau) = a_2\tau^2 + a_1\tau + a_0 < 0, \forall \tau \in [d_1, d_2]$ holds true if the following conditions are satisfied:

$$C_{1i} = f(d_i) < 0, \quad i = 1, 2, \tag{4}$$

$$C_{13} = -\frac{\alpha_{Mm}^2}{M^2} d_{12}^2 a_2 + f \left(d_1 + \frac{m-1}{M} d_{12} \right) < 0, \tag{5}$$

$$C_{14} = -\frac{(1-\alpha_{Mm})^2}{M^2} d_{12}^2 a_2 + f \left(d_1 + \frac{m}{M} d_{12} \right) < 0. \tag{6}$$

Proof. In the case of $a_2 > 0$, $f(\tau)$ is a convex function. It is clear as shown in Figure 2(a) that condition (4) guarantees $f(\tau) < 0$ for $\tau \in [d_1, d_2]$.

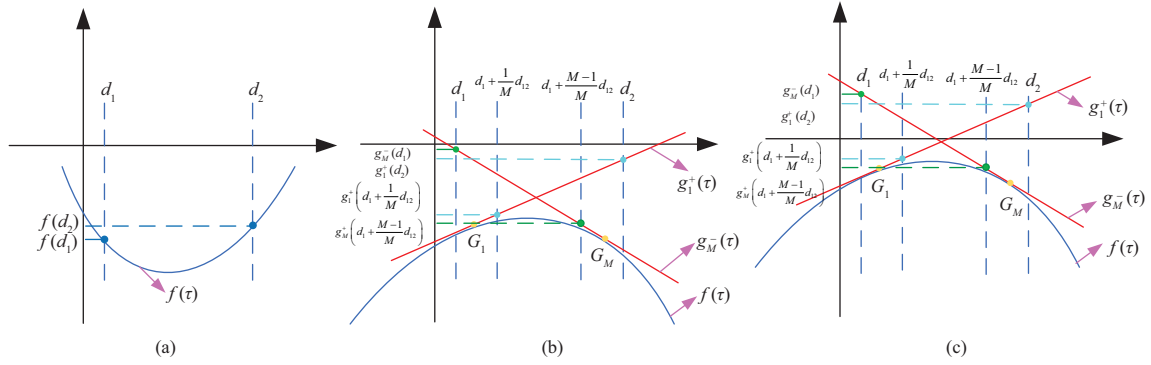


Figure 2 (Color online) Negative definite conditions of the quadratic function. (a) The case of $a_2 > 0$; (b) general case of $a_2 < 0$; (c) special case of $a_2 < 0$.

In the case of $a_2 < 0$, $f(\tau)$ is a concave function. The delay interval $[d_1, d_2]$ can be divided into M subintervals $[d_1 + \frac{m-1}{M}d_{12}, d_1 + \frac{m}{M}d_{12}]$, $m = 1, 2, \dots, M$, i.e.,

$$\begin{aligned}
 [d_1, d_2] &\triangleq \left[d_1, d_1 + \frac{1}{M}d_{12} \right) \cup \left[d_1 + \frac{1}{M}d_{12}, d_1 + \frac{2}{M}d_{12} \right) \\
 &\cup \dots \cup \left[d_1 + \frac{M-1}{M}d_{12}, d_2 \right],
 \end{aligned} \tag{7}$$

and then $f(\tau)$ can be represented as a piecewise function $f_m(\tau)$, $\tau \in [d_1 + \frac{m-1}{M}d_{12}, d_1 + \frac{m}{M}d_{12}]$, i.e.,

$$f(\tau) = \begin{cases} f_1(\tau), & \tau \in [d_1, d_1 + \frac{1}{M}d_{12}), \\ f_2(\tau), & \tau \in [d_1 + \frac{1}{M}d_{12}, d_1 + \frac{2}{M}d_{12}), \\ \vdots \\ f_M(\tau), & \tau \in [d_1 + \frac{M-1}{M}d_{12}, d_2]. \end{cases} \tag{8}$$

Let $\tau_0 \in [d_1 + \frac{m-1}{M}d_{12}, d_1 + \frac{m}{M}d_{12}]$ be any constant. The following equation is clearly true from Figures 2(b) and (c):

$$\begin{aligned}
 f_m(\tau) &\leq \dot{f}(\tau_0)(\tau - \tau_0) + f(\tau_0) \\
 &= (2a_2\tau_0 + a_1)\tau - a_2\tau_0^2 + a_0 \\
 &\triangleq g_m(\tau).
 \end{aligned} \tag{9}$$

It is found that the tangent line $g_m(\tau)$ is a linear function. Then $f_m(\tau) \leq g_m(\tau) < 0$ will hold for $\tau \in [d_1 + \frac{m-1}{M}d_{12}, d_1 + \frac{m}{M}d_{12}]$, i.e., $f(\tau) \leq g(\tau) < 0$ will hold for $\tau \in [d_1, d_2]$, if the following hold:

$$\begin{aligned}
 g_m \left(d_1 + \frac{m-1}{M}d_{12} \right) &= 2a_2\tau_0d_1 + a_1d_1 + 2a_2\tau_0 \frac{m-1}{M}d_{12} \\
 &\quad + a_1 \frac{m-1}{M}d_{12} - a_2\tau_0^2 + a_0 < 0,
 \end{aligned} \tag{10}$$

$$\begin{aligned}
 g_m \left(d_1 + \frac{m}{M}d_{12} \right) &= 2a_2\tau_0d_1 + a_1d_1 + 2a_2\tau_0 \frac{m}{M}d_{12} \\
 &\quad + a_1 \frac{m}{M}d_{12} - a_2\tau_0^2 + a_0 < 0.
 \end{aligned} \tag{11}$$

Let $\tau_0 = (d_1 + \frac{m-1}{M}d_{12}) + \frac{\alpha_{Mm}}{M}d_{12}$ with $\alpha_{Mm} \in [0, 1]$, $m = 1, 2, \dots, M$ be any constant. Eqs. (10) and (11) lead to (5) and (6), respectively, further yielding $f(\tau) < 0$ with $a_2 < 0$.

Remark 1. Existing quadratic convex frameworks are given in Table 2 [34–39]. Specifically, the comparisons between Lemma 1 and the previous ones are discussed as follows.

- The conditions in [34, 35] are only applicable to the case of $a_2 > 0$. If $a_2 < 0$, it is not valid.
- If set $M = 1$, $\alpha_{Mm} = 1$, conditions in Lemma 1 will reduce to those in [36, 37]:

Table 2 Existing quadratic convex frameworks

Refs.	Quadratic convex conditions
[34, 35]	$C_{1i} = f(d_i) < 0, i = 1, 2$
[36, 37]	$C_{2i} = f(d_i) < 0, C_{23} = -d_{12}^2 a_2 + f(d_1) < 0$
[38]	$C_{3i} = f(d_i) < 0, C_{33} = -\frac{1}{M^2} d_{12}^2 a_2 + f(\frac{m-1}{M} d_{12}) < 0, C_{34} = f(\frac{m}{M} d_{12}) < 0$
[39]	$C_{4i} = f(d_i) < 0, C_{43} = -\alpha^2 d_{12}^2 a_2 + f(d_1) < 0, C_{44} = -(1 - \alpha)^2 d_{12}^2 a_2 + f(d_2) < 0$

For the case of $a_2 \geq 0$ in Figure 2(a), conditions of Lemma 1 and [36, 37] are all simplified as $C_{2i} = f(d_i) < 0$ due to $C_{23} \leq C_{21}, C_{13} \leq C_{11} = C_{21}, C_{14} \leq C_{12} = C_{22}$.

For the case of $a_2 < 0$, it follows from Figures 2(b) and (c) that, if the slope of the tangent line at any point in $[d_1, d_2]$ (such as G_M) is no greater than zero, the negative definite condition $g_M^-(d_1) < 0$ in [36, 37] will be more demanding than $g_M^-(d_1 + \frac{M-1}{M} d_{12}) < 0$ in Lemma 1 (specifically, for the case in Figure 2(c), $g_M^-(d_1) < 0$ no longer holds, while $g_M^-(d_1 + \frac{M-1}{M} d_{12}) < 0$ in Lemma 1 still guarantees that $f(\tau) < 0$). A more rigorous explanation is as follows:

$$\begin{aligned} \mathcal{E}_1 &= C_{23} - C_{13} \\ &= [-d_{12}^2 a_2 + f(d_1)] - \left[-\frac{(\alpha_{Mm})^2}{M^2} d_{12}^2 a_2 + f\left(d_1 + \frac{m-1}{M} d_{12}\right) \right] \\ &\geq -d_{12}^2 a_2 \left\{ 1 - \left[\frac{\alpha_{Mm} + (m-1)}{M} \right]^2 \right\} > 0, \end{aligned} \tag{12}$$

under the condition of $\dot{f}(\tau)|_{\tau_0=d_1+\frac{m-1}{M}d_{12}+\frac{\alpha_{Mm}}{M}d_{12}} = 2a_2(d_1 + \frac{m-1}{M}d_{12} + \frac{\alpha_{Mm}}{M}d_{12}) + a_1 \leq 0$, which means that Eq. (5) is more relaxed than that in [36, 37]. Similarly, if the slope of the tangent line at any point in $[d_1, d_2]$ (such as G_1) is greater than zero, the negative definite condition $g_1^+(d_2) < 0$ in [36, 37] will be more demanding than $g_1^+(d_1 + \frac{1}{M}d_{12}) < 0$ in Lemma 1 from Figures 2(b) and (c). Algebraically,

$$\begin{aligned} \mathcal{E}_2 &= C_{23} - C_{14} \\ &= [-d_{12}^2 a_2 + f(d_1)] - \left[-\frac{(1 - \alpha_{Mm})^2}{M^2} d_{12}^2 a_2 + f\left(d_1 + \frac{m}{M} d_{12}\right) \right] \\ &< -d_{12}^2 a_2 \left\{ 1 - \left[\frac{1 - \alpha_{Mm} - m}{M} \right]^2 \right\} > 0 \end{aligned} \tag{13}$$

under the condition of $2a_2(d_1 + \frac{m-1}{M}d_{12} + \frac{\alpha_{Mm}}{M}d_{12}) + a_1 > 0$. By choosing suitable α_{Mm} and M , one can obtain $C_{23} > C_{14}$, which means that Eq. (6) is also more relaxed than that in [36, 37].

- If set $\alpha_{Mm} = 1$, conditions in Lemma 1 will reduce to those in [38].
- If set $M = 1$, conditions in Lemma 1 will degenerate to those in [39]; in other words, Lemma 1 also covers the method in [39] as a special case.

Remark 2. The novel quadratic convex framework in Lemma 1 is with bigger freedom due to the introduction of adjustable free parameters M and α_{Mm} , which are beneficial to reduce conservatism.

- As M increases, the combination of all the straight lines $g_m(\tau_m), m = 1, 2, \dots, M$ gradually approaches to the curve line $f(\tau)$, whereas the values of $-\frac{\alpha_{Mm}^2}{M^2} d_{12}^2 a_2, -\frac{(1-\alpha_{Mm})^2}{M^2} d_{12}^2 a_2$ reduce. Therefore, the inequality constraints (5) and (6) in Lemma 1 become more relaxed as M increases and the conservatism tends to disappear for sufficiently big M .

- As α_{Mm} changes within $[0, 1]$, the sizes of two positive terms $-\frac{\alpha_{Mm}^2}{M^2} d_{12}^2 a_2$ and $-\frac{(1-\alpha_{Mm})^2}{M^2} d_{12}^2 a_2$ associated with $f(d_1 + \frac{m-1}{M}d_{12})$ and $f(d_1 + \frac{m}{M}d_{12})$ change for a fixed M . Therefore, taking suitable value of α_{Mm} , the conservatism is further reduced.

Now, we are ready to derive the stability criteria of the cyber-physical microgrid system based on the abovementioned quadratic convex framework together with some new tools in the subsequent.

4 Stability analysis for LFC microgrid system

First of all, some lemmas are introduced, which are helpful to derive the stability analysis conditions.

Lemma 2 ([29]). Let $c < d, R = R^T > 0$. Then

$$-\int_c^d \dot{x}(s)^T R \dot{x}(s) ds \leq \sum_{l=1}^3 (2l-1) \Gamma_l^T R \Gamma_l, \tag{14}$$

where

$$\begin{aligned} \Gamma_1 &= x(d) - x(c), \quad \Gamma_2 = x(d) + x(c) - \frac{2}{d-c} \int_c^d x(s) ds, \\ \Gamma_3 &= x(d) - x(c) + \frac{6}{d-c} \int_c^d x(s) ds - \frac{12}{(d-c)^2} \int_c^d \int_\theta^d x(s) ds d\theta. \end{aligned} \tag{15}$$

Lemma 3 ([31]). Let $X_1, X_2 \in \mathbb{R}^{m \times m}$ be real symmetric positive definite matrices, $\varpi_2, \varpi_3 \in \mathbb{R}^m$, and a scalar $\beta \in [0, 1]$. Then for any $Y_1, Y_2 \in \mathbb{R}^{m \times m}$, the following inequality holds:

$$\begin{aligned} \frac{1}{\beta} \varpi_2^T X_1 \varpi_2 + \frac{1}{1-\beta} \varpi_3^T X_2 \varpi_3 &\geq (2-\beta) \varpi_2^T X_1 \varpi_2 + (1+\beta) \varpi_3^T X_2 \varpi_3 \\ &\quad + \text{sym}\{(1-\beta) \varpi_2^T Y_1^T + \beta \varpi_3^T Y_2^T\} \\ &\quad - \beta Y_1 X_1^{-1} Y_1^T - (1-\beta) Y_2 X_2^{-1} Y_2^T. \end{aligned} \tag{16}$$

For simplicity of presentation, the following notations are used:

$$\begin{aligned} \rho(a, b, t) &= \int_{t-a}^{t-b} \frac{x(s)}{a-b} ds, \\ \sigma(a, b, t) &= \int_{t-a}^{t-b} \int_r^{t-b} \frac{x(s)}{(a-b)^2} ds dr, \\ \eta_0(t) &= \text{col}\{x(t), d_1 \rho(d_1, 0, t), d_{12} \rho(d_2, d_1, t), d_1^2 \sigma(d_1, 0, t), d_{12}^2 \sigma(d_2, d_1, t)\}, \\ \eta_1(t, s) &= \text{col}\left\{x(s), x(t), \int_s^{t-d_1} x^T(r) dr, \int_{t-d_2}^s x^T(r) dr\right\}, \\ \xi_1(t) &= \text{col}\{x(t), x(t-d_1), x(t-d(t)), x(t-d_2)\}, \\ \xi_2(t) &= \text{col}\{\rho(d_1, 0, t), \rho(d(t), d_1, t), \rho(d_2, d(t), t)\}, \\ \xi_3(t) &= \text{col}\{\sigma(d_1, 0, t), \sigma(d(t), d_1, t), \sigma(d_2, d(t), t)\}, \\ \xi_4(t) &= \text{col}\{(d(t)-d_1) \rho(d(t), d_1, t), (d_2-d(t)) \rho(d_2, d(t), t)\}, \\ \xi(t) &= \text{col}\{\xi_1(t), \xi_2(t), \xi_3(t), \xi_4(t)\}, \\ e_k &= [0_{n \times (k-1)n}, I_n, 0_{n \times (12-k)n}], \quad k = 1, 2, \dots, 12. \end{aligned} \tag{17}$$

The following delay-dependent stability criterion is stated for the cyber-physical LFC microgrid based on the augmented LKF together with the relaxed quadratic convex framework, in which the effect of free parameters M and α_{Mm} is described.

Theorem 1. For given constants $d_1, d_2 > 0$, the adjustable parameter $\alpha_{Mm}, m = 1, 2, \dots, M$, and a positive integer M , the LFC microgrid system with time-varying delay $d(t)$ will be globally asymptotically stable if there exist real matrices $P \in \mathbb{S}_+^{5n}, Q_1 \in \mathbb{S}_+^n, Q_2 \in \mathbb{S}_+^{4n}, R_1 \in \mathbb{S}_+^n, R_2 \in \mathbb{S}_+^n$, any matrices $U_1, U_2 \in \mathbb{R}^{2n \times n}$ and $Y_1, Y_2 \in \mathbb{R}^{12n \times 3n}$ such that the following inequalities hold:

$$\begin{bmatrix} \Pi(d_1) & Y_2 \\ * & -\tilde{R}_2 \end{bmatrix} < 0, \tag{18}$$

$$\begin{bmatrix} \Pi(d_2) & Y_1 \\ * & -\tilde{R}_2 \end{bmatrix} < 0, \tag{19}$$

$$\left\{ \begin{aligned} & \left[\begin{array}{cc} -\frac{\alpha_{Mm}^2}{M^2}d_{12}^2\Pi_0 + \Pi(d_1) & Y_2 \\ * & -\tilde{R}_2 \end{array} \right] < 0, \quad m = 1, \\ & \left[\begin{array}{ccc} \Pi_1(m, \alpha_{Mm}) & Y_1 & Y_2 \\ * & -\frac{M}{m-1}\tilde{R}_2 & 0 \\ * & * & -\frac{M}{M-m+1}\tilde{R}_2 \end{array} \right] < 0, \quad 2 \leq m \leq M, \end{aligned} \right. \quad (20)$$

$$\left\{ \begin{aligned} & \left[\begin{array}{ccc} \Pi_2(m, \alpha_{Mm}) & Y_1 & Y_2 \\ * & -\frac{M}{m}\tilde{R}_2 & 0 \\ * & * & -\frac{M}{M-m}\tilde{R}_2 \end{array} \right] < 0, \quad 1 \leq m < M, \\ & \left[\begin{array}{cc} -\frac{(1-\alpha_{Mm})^2}{M^2}d_{12}^2\Pi_0 + \Pi(d_2) & Y_1 \\ * & -\tilde{R}_2 \end{array} \right] < 0, \quad m = M, \end{aligned} \right. \quad (21)$$

where

$$\begin{aligned} \Pi_0 &= \frac{1}{2} \frac{\partial^2 \Pi(\tau)}{\partial \tau^2} \\ &= \text{sym}\{\text{col}\{0, 0, 0, 0, e_9 + e_{10}\}PH_1\} + \text{sym}\{\text{col}\{0, 0, e_9 + e_{10}, -e_9 - e_{10}\}Q_2H_5\}, \\ \Pi(\tau) &= \text{sym}\{H_2^T(\tau)PH_1\} \\ &\quad + e_1^T Q_1 e_1 - e_2^T Q_1 e_2 + H_3^T Q_2 H_3 - H_4^T Q_2 H_4 + \text{sym}\{H_6^T(\tau)Q_2H_5\} \\ &\quad + A_c^T(d_1^2 R_1 + d_{12}^2 R_2)A_c - \varpi_1^T \tilde{R}_1 \varpi_1 \\ &\quad - [(2 - \beta)\varpi_2^T \tilde{R}_2 \varpi_2 + (1 + \beta)\varpi_3^T \tilde{R}_2 \varpi_3 + \text{sym}\{(1 - \beta)\varpi_2^T Y_1^T + \beta\varpi_3^T Y_2^T\}] \\ &\quad + \text{sym}\{[e_6^T, e_{11}^T]U_1[(\tau - d_1)e_6 - e_{11}]\} \\ &\quad + \text{sym}\{[e_7^T, e_{12}^T]U_2[(d_2 - \tau)e_7 - e_{12}]\}, \\ \Pi_1(m, \alpha_{Mm}) &= -\frac{\alpha_{Mm}^2}{M^2}d_{12}^2\Pi_0 + \Pi\left(d_1 + \frac{m-1}{M}d_{12}\right), \\ \Pi_2(m, \alpha_{Mm}) &= -\frac{(1-\alpha_{Mm})^2}{M^2}d_{12}^2\Pi_0 + \Pi\left(d_1 + \frac{m}{M}d_{12}\right), \\ H_1 &= \text{col}\{A_c, e_1 - e_2, e_2 - e_4, d_1(e_1 - e_5), d_{12}e_2 - e_{11} - e_{12}\}, \\ H_2(\tau) &= \text{col}\{e_1, d_1e_5, e_{11} + e_{12}, d_1^2e_8, (\tau - d_1)^2e_9 + (d_2 - \tau)^2e_{10} + (d_2 - \tau)e_{11}\}, \\ H_3 &= \text{col}\{e_2, e_1, 0, e_{11} + e_{12}\}, \\ H_4 &= \text{col}\{e_4, e_1, e_{11} + e_{12}, 0\}, \\ H_5 &= \text{col}\{0, A_c, e_2, -e_4\}, \\ H_6(\tau) &= \text{col}\{e_{11} + e_{12}, d_{12}e_1, (\tau - d_1)^2e_9 + (d_2 - \tau)^2e_{10} + (d_2 - \tau)e_{11}, \\ &\quad d_{12}(e_{11} + e_{12}) - [(\tau - d_1)^2e_9 + (d_2 - \tau)^2e_{10} + (d_2 - \tau)e_{11}]\}, \\ \varpi_l &= \text{col}\{e_l - e_{l+1}, e_l + e_{l+1} - 2e_{l+4}, e_l - e_{l+1} + 6e_{l+4} - 12e_{l+7}\}, \quad l = 1, 2, 3, \\ \tilde{R}_i &= \text{diag}\{R_i, 3R_i, 5R_i\}, \quad i = 1, 2, \\ \beta &= \frac{(\tau - d_1)}{d_{12}}, \quad \tau \triangleq d(t), \\ A_c &= Ae_1 + A_d e_3. \end{aligned} \quad (22)$$

Proof. Construct the following LKF candidate:

$$V(t, x(t), \dot{x}(t)) = V_1(t, x(t)) + V_2(t, x(t)) + V_3(t, \dot{x}(t)), \quad (23)$$

where

$$V_1(t, x(t)) = \eta_0^T(t)P\eta_0(t), \quad (24)$$

$$V_2(t, x(t)) = \int_{t-d_1}^t x^T(s)Q_1x(s)ds + \int_{t-d_2}^{t-d_1} \eta_1^T(t, s)Q_2\eta_1(t, s)ds, \quad (25)$$

$$V_3(t, \dot{x}(t)) = d_1 \int_{-d_1}^0 \int_{t+r}^t \dot{x}^T(s)R_1\dot{x}(s)dsdr + d_{12} \int_{-d_2}^{-d_1} \int_{t+r}^t \dot{x}^T(s)R_2\dot{x}(s)dsdr. \tag{26}$$

The time derivative of $V(t, x_t, \dot{x}_t)$ along the trajectories of LFC microgrid system can be obtained:

$$\dot{V}(t, x(t), \dot{x}(t)) = \dot{V}_1(t, x(t)) + \dot{V}_2(t, x(t)) + \dot{V}_3(t, \dot{x}(t)), \tag{27}$$

where

$$\dot{V}_1(t, x(t)) = \xi^T(t)\text{sym}\{H_2^T(\tau)PH_1\}\xi(t), \tag{28}$$

$$\begin{aligned} \dot{V}_2(t, x(t)) &= x^T(t)Q_1x(t) - x^T(t-d_1)Q_1x(t-d_1) + \eta_1^T(t, t-d_1)Q_2\eta_1(t, t-d_1) \\ &\quad - \eta_1^T(t, t-d_2)Q_2\eta_1(t, t-d_2) + 2 \int_{t-d_2}^{t-d_1} \eta_1^T(t, s)Q_2 \frac{\partial \eta_1(t, s)}{\partial t} ds, \end{aligned} \tag{29}$$

$$\dot{V}_3(t, \dot{x}(t)) = \dot{x}^T(t)(d_1^2R_1 + d_{12}^2R_2)\dot{x}(t) - J_1 - J_2. \tag{30}$$

Based on Lemmas 2 and 3, and letting $\beta = \frac{d(t)-d_1}{d_{12}}$, then J_1 and J_2 are respectively estimated as follows:

$$J_1 = d_1 \int_{t-d_1}^t \dot{x}^T(s)R_1\dot{x}(s)ds \geq \xi^T(t)\varpi_1^T \tilde{R}_1 \varpi_1 \xi(t), \tag{31}$$

$$\begin{aligned} J_2 &= d_{12} \int_{t-d(t)}^{t-d_1} \dot{x}^T(s)R_2\dot{x}(s)ds + d_{12} \int_{t-d_2}^{t-d(t)} \dot{x}^T(s)R_2\dot{x}(s)ds \\ &\geq \xi^T(t) \left[\frac{1}{\beta} \varpi_2^T \tilde{R}_2 \varpi_2 + \frac{1}{1-\beta} \varpi_3^T \tilde{R}_2 \varpi_3 \right] \xi(t) \\ &\geq \xi^T(t) [(2-\beta)\varpi_2^T \tilde{R}_2 \varpi_2 + (1+\beta)\varpi_3^T \tilde{R}_2 \varpi_3 \\ &\quad + \text{sym}\{(1-\beta)\varpi_2^T Y_1^T + \beta\varpi_3^T Y_2^T\} \\ &\quad - \beta Y_1 \tilde{R}_2^{-1} Y_1^T - (1-\beta)Y_2 \tilde{R}_2^{-1} Y_2^T] \xi(t). \end{aligned} \tag{32}$$

For any real matrices U_1, U_2 , the following holds obviously:

$$\begin{aligned} u_1 &= 2[\rho^T(d(t), d_1, t), (d(t)-d_1)\rho(d(t), d_1, t)]U_1 \\ &\quad \times [(d(t)-d_1) \int_{t-d(t)}^{t-d_1} \frac{x(s)}{d(t)-d_1} ds - \int_{t-d(t)}^{t-d_1} x(s)ds] \\ &= \xi^T(t)\text{sym}\{[e_6^T, e_{11}^T]U_1[(\tau-d_1)e_6 - e_{11}]\}\xi(t) = 0, \end{aligned} \tag{33}$$

$$\begin{aligned} u_2 &= 2[\rho^T(d_2, d(t), t), (d_2-d(t))\rho(d_2, d(t), t)]U_2 \\ &\quad \times [(d_2-d(t)) \int_{t-d_2}^{t-d(t)} \frac{x(s)}{d_2-d(t)} ds - \int_{t-d_2}^{t-d(t)} x(s)ds] \\ &= \xi^T(t)\text{sym}\{[e_7^T, e_{12}^T]U_2[(d_2-\tau)e_7 - e_{12}]\}\xi(t) = 0. \end{aligned} \tag{34}$$

According to (23)–(34), one has

$$\begin{aligned} \dot{V}(t, x(t), \dot{x}(t)) &= \dot{V}_1(t, x(t)) + \dot{V}_2(t, x(t)) + \dot{V}_3(t, \dot{x}(t)) + u_1 + u_2 \\ &\leq \xi^T(t)[\Pi(\tau) + \beta Y_1 \tilde{R}_2^{-1} Y_1^T + (1-\beta)Y_2 \tilde{R}_2^{-1} Y_2^T] \xi(t), \end{aligned} \tag{35}$$

where $\xi^T(t)[\Pi(\tau) + \beta Y_1 \tilde{R}_2^{-1} Y_1^T + (1-\beta)Y_2 \tilde{R}_2^{-1} Y_2^T] \xi(t) \triangleq \xi^T(t)[\Pi(\tau) + \Pi_\beta(\tau)] \xi(t)$ satisfies the quadratic function defined in Lemma 1 with $\tau \triangleq d(t)$, $a_2 = \xi^T(t)\Pi_0 \xi(t)$ defined in (22), and a_1, a_0 are τ itself independent symmetric matrices. Thus, applying the novel quadratic convex approach in Lemma 1, the following inequality:

$$\xi^T(t)[\Pi(\tau) + \Pi_\beta(\tau)] \xi(t) < 0 \tag{36}$$

holds if the inequalities below for any $\beta \in [0, 1]$ are satisfied:

$$\Pi(d_1) + \Pi_\beta(d_1) < 0, \tag{37}$$

$$\Pi(d_2) + \Pi_\beta(d_2) < 0, \tag{38}$$

$$-\frac{\alpha_{Mm}^2}{M^2}d_{12}^2\Pi_0 + \Pi\left(d_1 + \frac{m-1}{M}d_{12}\right) + \Pi_\beta\left(d_1 + \frac{m-1}{M}d_{12}\right) < 0, \tag{39}$$

$$-\frac{(1-\alpha_{Mm})^2}{M^2}d_{12}^2\Pi_0 + \Pi\left(d_1 + \frac{m}{M}d_{12}\right) + \Pi_\beta\left(d_1 + \frac{m}{M}d_{12}\right) < 0. \tag{40}$$

Specifically, it follows from Schur complement that

$$\begin{cases} (18) \Leftrightarrow (37) \\ (19) \Leftrightarrow (38) \\ (20) \Leftrightarrow (39) \\ (21) \Leftrightarrow (40) \end{cases} \Rightarrow \Pi(\tau) + \Pi_\beta(\tau) < 0 \Rightarrow \xi^T(t)[\Pi(\tau) + \Pi_\beta(\tau)]\xi(t) < 0 \Rightarrow \dot{V}(t, x(t), \dot{x}(t)) < 0. \tag{41}$$

Thus, the cyber-physical LFC microgrid system will be globally asymptotically stable if Eqs. (18)–(21) hold.

Remark 3. Theorem 1 is expected to present the less conservative stability analysis condition for the cyber-physical LFC microgrids. The novelties are shown from the following two aspects.

- Compared with the LKF construction used for microgrid stability in [19, 20] with a quadratic term only depending on the instantaneous state vector, $V_1(t, x(t))$ and $V_2(t, x(t))$ in (24) and (25) are augmented LKF candidates, i.e., $\eta_0^T(t)P\eta_0(t)$ with $\eta_0(t)$ including $x(t)$, $d_1\rho(d_1, 0, t)$, $d_{12}\rho(d_2, d_1, t)$, $d_1^2\sigma(d_1, 0, t)$, and $d_{12}^2\sigma(d_2, d_1, t)$. It fully benefits from the second-order Bessel-Legendre inequality. $\eta_1^T(t, s)Q_2\eta_1(t, s)$ with $\eta_1(t, s)$ also including more system states and integral terms makes the system state and some delayed states coupled closely, possibly enhancing the feasibility of the related LMIs in the stability criteria and being helpful to derive less conservative results.

- The result of Theorem 1 contains not only the quadratic terms of $d(t)$, but also its inverse terms. Hence, the novel quadratic convex framework in Lemma 1, reciprocally convex combination in Lemma 3 are comprehensively used. It is worth mentioning that Eqs. (37)–(40) are parameter dependent, which are derived by the α_{Mm} , M -dependent quadratic convex framework, and β -dependent reciprocally convex combination with β being usually related to the time-varying delay $d(t)$. Therefore, additional degrees of freedom are introduced and the conservatism of Theorem 1 is further reduced.

Remark 4. Different from the results in [19, 21] that only apply to the delayed microgrid system with $\dot{d}(t) < 1$, Theorem 1 is suitable for the system with no knowledge of the $\dot{d}(t)$ constraint. When it comes to system limitations or uncertainties that make the delay derivative range unavailable, the results in [19, 21] cannot be applicable anymore, but Theorem 1 is still available.

Two special cases are given next. The first one is that if Eq. (36) is handled by using Lemma 1 with $M = 1$, then Corollary 1 will be directly obtained; the second is Corollary 2 based on Lemma 1 with $M = 1, \alpha_{Mm} = 1$.

Corollary 1. For given constants $d_1, d_2 > 0$ and fixed α freely selected within $[0, 1]$, the LFC microgrid system with time-varying delay $d(t)$ will be globally asymptotically stable if there exist real matrices $P \in \mathbb{S}_+^{5n}, Q_1 \in \mathbb{S}_+^n, Q_2 \in \mathbb{S}_+^{4n}, R_1 \in \mathbb{S}_+^n, R_2 \in \mathbb{S}_+^n$, any matrices $U_1, U_2 \in \mathbb{R}^{2n \times n}$ and $Y_1, Y_2 \in \mathbb{R}^{12n \times 3n}$ such that the following inequalities hold:

$$\begin{bmatrix} \Pi(d_1) - \lambda_i^2 d_{12}^2 \Pi_0 & Y_2 \\ * & -\tilde{R}_2 \end{bmatrix} < 0, \quad i = 1, 2, \tag{42}$$

$$\begin{bmatrix} \Pi(d_2) - \lambda_j^2 d_{12}^2 \Pi_0 & Y_1 \\ * & -\tilde{R}_2 \end{bmatrix} < 0, \quad j = 3, 4, \tag{43}$$

where $\lambda_1 = \lambda_3 = 0, \lambda_2 = \alpha, \lambda_4 = 1 - \alpha$ and the other notations are defined the same as in (22).

Corollary 2. For given scalars $d_1, d_2 > 0$, the LFC microgrid system with time-varying delay $d(t)$ will be globally asymptotically stable if there exist real matrices $P \in \mathbb{S}_+^{5n}, Q_1 \in \mathbb{S}_+^n, Q_2 \in \mathbb{S}_+^{4n}, R_1 \in \mathbb{S}_+^n, R_2 \in \mathbb{S}_+^n$, any matrices $U_1, U_2 \in \mathbb{R}^{2n \times n}$ and $Y_1, Y_2 \in \mathbb{R}^{12n \times 3n}$ such that the following inequalities hold:

$$\begin{bmatrix} \Pi(d_1) - \bar{\lambda}_i^2 d_{12}^2 \Pi_0 & Y_2 \\ * & -\tilde{R}_2 \end{bmatrix} < 0, \quad i = 1, 2, \tag{44}$$

Table 3 AMDBs and NVs for different d_1, M and α

Method	AMDB				NV	M	α ($\alpha = \alpha_{11}$ or $\alpha = \alpha_{21} = 1 - \alpha_{22}$)
	$d_1=0$	$d_1=0.3$	$d_1=0.7$	$d_1=1.0$			
[28]	1.59	2.01	2.41	2.62	49	–	–
[29]	1.64	2.13	2.70	2.92	96	–	–
[30]	1.80	2.19	2.58	2.79	73	–	–
[31]	1.86	2.28	2.69	2.89	93	–	–
[39]	1.74	2.24	2.84	3.11	371	–	1.0
[39]	1.88	2.50	2.98	3.20	371	–	0.6
[39]	1.97	2.54	2.96	3.18	371	–	0.4
[40]	1.98	2.50	2.95	3.20	424	–	–
[40]	2.48	2.84	3.18	3.40	424	1	–
[40]	2.52	2.88	3.22	3.43	424	2	–
Corollary 2	1.86	2.32	2.92	3.18	404	1	1.0
Corollary 1	2.00	2.56	3.03	3.25	404	1	0.6
Corollary 1	2.14	2.73	3.06	3.24	404	1	0.4
Corollary 1	2.17	2.69	3.03	3.19	404	1	0.2
Corollary 1	2.10	2.59	2.98	3.15	404	1	0.0
Theorem 1	2.07	2.69	3.05	3.26	404	2	1.0
Theorem 1	2.21	2.79	3.11	3.29	404	2	0.6
Theorem 1	2.23	2.80	3.12	3.30	404	2	0.4
Theorem 1	2.21	2.78	3.12	3.30	404	2	0.2
Theorem 1	2.17	2.73	3.10	3.28	404	2	0.0

$$\begin{bmatrix} \Pi(d_2) & Y_1 \\ * & -\tilde{R}_2 \end{bmatrix} < 0, \tag{45}$$

where $\bar{\lambda}_1 = 0, \bar{\lambda}_2 = 1$, and the other notations are defined the same as in (22).

The detailed process of calculating delay margins for the microgrid system is given step by step as follows.

Step 1. The system parameters are chosen to obtain the state space model.

Step 2. A series of values for the PI controller gain and the delay lower bound d_1 are selected. This prepares for the delay margin calculation.

Step 3. The stability margin is calculated by using the LMIs in Theorem 1, Corollary 1 or Corollary 2, and the admitted maximum delay bounds d_2 are obtained. The conservativeness of the proposed method can be compared.

5 Simulation

In this section, two types of simulations including a typical numerical example and an actual microgrid system example are carried out. The effectiveness of the theoretical methods is verified, and the superiority in the actual engineering is demonstrated.

5.1 A well-known numerical example

Consider the system with the following matrices [28–31, 39, 40]:

$$A = \begin{bmatrix} 0 & 1 \\ -10 & -1 \end{bmatrix}, \quad A_d = \begin{bmatrix} 0 & 0.1 \\ 0.1 & 0.2 \end{bmatrix}.$$

The AMDBs d_2 and the number of decision variables (NVs) with respect to various d_1 and adjustable parameters α_{Mm}, M are listed in Table 3, in which the results by Corollaries 1 and 2, and Theorem 1 with $\alpha = 1$ respectively represent ones of the quadratic convex framework processing in [36–39] from Table 2. The following observations are summarized.

Table 4 AMDBs based on methods in this paper and [21] for different MGCC gains

R_{ic}	Method	AMDB							
		$R_{pc}=1$	$R_{pc}=2$	$R_{pc}=3$	$R_{pc}=4$	$R_{pc}=5$	$R_{pc}=6$	$R_{pc}=7$	$R_{pc}=8$
0.2	[21]	9.864	12.469	12.653	11.087	9.359	7.959	6.876	6.031
	Corollary 2	9.867	12.493	12.785	11.403	9.719	8.321	7.226	6.363
	Corollary 1	9.868	12.495	12.786	11.405	9.721	8.323	7.228	6.365
	Theorem 1	9.869	12.496	12.789	11.409	9.730	8.336	7.241	6.376
0.4	[21]	5.246	7.105	8.249	8.575	8.159	7.385	6.578	5.861
	Corollary 2	5.246	7.117	8.272	8.627	8.304	7.604	6.828	6.124
	Corollary 1	5.247	7.118	8.274	8.628	8.305	7.605	6.830	6.125
	Theorem 1	5.248	7.119	8.279	8.631	8.310	7.610	6.837	6.132
0.6	[21]	3.656	5.028	6.057	6.678	6.859	6.636	6.173	5.637
	Corollary 2	3.656	5.036	6.072	6.700	6.903	6.737	6.332	5.833
	Corollary 1	3.656	5.035	6.072	6.702	6.905	6.739	6.333	5.835
	Theorem 1	3.657	5.039	6.077	6.706	6.907	6.743	6.336	5.837
0.8	[21]	2.852	3.933	4.811	5.442	5.802	5.876	5.697	5.358
	Corollary 2	2.853	3.938	4.820	5.458	5.825	5.920	5.786	5.493
	Corollary 1	2.853	3.938	4.821	5.460	5.828	5.922	5.789	5.495
	Theorem 1	2.853	3.939	4.822	5.463	5.832	5.926	5.925	5.886
1.0	[21]	2.368	3.257	4.013	4.602	5.007	5.211	5.213	5.043
	Corollary 2	2.368	3.261	4.019	4.612	5.023	5.236	5.260	5.129
	Corollary 1	2.368	3.260	4.018	4.612	5.026	5.240	5.262	5.132
	Theorem 1	2.369	3.261	4.020	4.616	5.029	5.242	5.265	5.133

- The produced AMDBs by Theorem 1, Corollaries 1 and 2 are obviously bigger than those in [28–31, 39] (under the same α settings) for both $M = 1$ and $M = 2$, which shows that the results obtained by our methods are much less conservative than those from the abovementioned literature.

- Theorem 1 provides bigger AMDBs than Corollaries 1 and 2; i.e., the conservatism is further reduced if M increases and α is appropriate, which verifies the effectiveness of Lemma 1 and the statement of Remark 2 again. In addition, compared with Corollaries 1 and 2, no additional decision variables are introduced to reduce the conservativeness in Theorem 1.

- Compared with Corollary 2, Corollary 1 with a specific value of α leads to a more conservative result (for example, the case that $d_1 = 1.0$ and $\alpha = 0.0$). It illustrates that there is no requirement for all α within $[0, 1]$ and the conditions in Lemma 1 are relaxed than those of the traditional quadratic convex framework.

- The AMDB results in the work of [40] are better than those of Theorem 1 in some cases; however, they utilize more decision variables than those in this paper, meaning that the computational complexity in [40] is higher. It is interesting to see that Theorem 1 can be complementary with that in [40].

5.2 LFC microgrid example

The cyber-physical microgrid system parameters taken from [17] are as follows: $M = 10, D = 1, R_{es} = 1, T_{es} = 1, R_{fc} = 1, T_{fc} = 4, R_{mt} = 0.04, R_{pl} = 1, R_{il} = 1$.

For different MGCC gains, the AMDB comparison results are given in Table 4 according to Theorem 1, Corollaries 1 and 2 in this paper, and the method in [21], where the delay lower bound $d_1 = 0$, the value of α in Corollary 1 and Theorem 1 is 0.52, and M in Theorem 1 is selected as 2. Figure 3 shows the relationship between delay margins by using Theorem 1 and MGCC gains R_{pc} and R_{ic} .

Based on the results in Table 4 and Figure 3, the following observations can be summarized.

- Theorem 1, Corollaries 1 and 2 in this paper provide bigger AMDB d_2 than the method reported in [21] as shown in Table 4, which means that the contributions of the tighter inequality and the more general LKF to reduce conservatism are well reflected by using Lemma 1 and its degenerate form to handle $d^2(t)$ -dependent terms.

- For the fixed MGCC proportional gain R_{pc} , AMDB d_2 decreases as R_{ic} increases, implying that the decrease of the integral gain R_{ic} results in a stable cyber-physical microgrid system. In addition, for a fixed R_{ic} , with the increase of R_{pc} , the AMDB d_2 increases first and then decreases. It just shows from

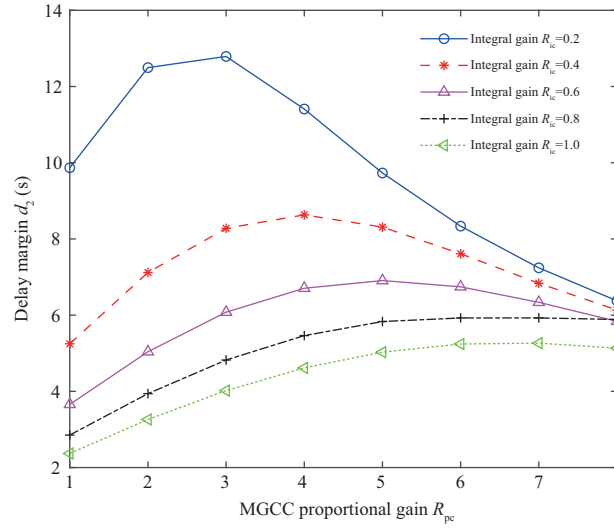


Figure 3 (Color online) Relationship between delay margin d_2 and MGCC gains R_{pc} and R_{ic} .

Table 5 AMDB comparison for different MGCC gains

R_{ic}	Method	AMDB		
		$R_{pc}=0.1$	$R_{pc}=0.6$	$R_{pc}=1.0$
0.1	[18]	10.04	11.20	15.86
	[20]	11.49	15.67	17.98
	Theorem 1	11.58	15.92	18.44
0.2	[18]	4.81	4.95	6.96
	[20]	5.89	8.17	9.71
	Theorem 1	5.92	8.25	9.86
0.4	[18]	2.38	2.73	3.32
	[20]	3.13	4.32	5.19
	Theorem 1	3.14	4.34	5.24
0.6	[18]	1.60	1.76	2.19
	[20]	2.21	3.02	3.62
	Theorem 1	2.22	3.03	3.65
0.8	[18]	1.1	1.38	1.65
	[20]	1.76	2.36	2.83
	Theorem 1	1.76	2.37	2.84

Figure 3 that the method has certain guiding significance for the determination of delay requirements and the design of load frequency controller for the cyber-physical microgrid system.

- Compared with Corollaries 1 and 2, Theorem 1 successfully reduces the conservatism by increasing the number of delay subinterval M and choosing suitable value of α . It verifies the contribution and advantage of the proposed quadratic convex framework in Lemma 1.

Moreover, the AMDB based on Theorem 1 and the methods in [18, 20] for different R_{pc} and R_{ic} are presented in Table 5. It can be seen that larger AMDBs are obtained by Theorem 1 in this paper; especially in the case that the proportional gain R_{pc} increases and the integral gain R_{ic} decreases, it is more obvious and consistent with the trend in Table 4. It again demonstrates the less conservatism of our approach than the standard tools mentioned above.

To illustrate the rationality of theoretical stability results of the microgrid system, two cases are verified using the time-domain simulation with initial frequency deviation being 0.

- In the case of $R_{pc} = 5, R_{ic} = 0.2, d(t) \in [0, 9.730]$, randomly set the time-varying delay as $d_1(t) = \frac{9.730}{2} \sin(\frac{4}{9.730}t) + \frac{9.730}{2}$ and $d_2(t) = \frac{9.730}{2} \sin(\frac{1}{9.730}t) + \frac{9.730}{2}$.

- In the case of $R_{pc} = 4, R_{ic} = 0.6, d(t) \in [0, 6.706]$, randomly set the time-varying delay as $d_3(t) = \frac{6.706}{4} \sin(\frac{1}{6.706}t) + \frac{6.706}{4}$ and $d_4(t) = \frac{6.706}{4} \sin(\frac{12}{6.706}t) + \frac{6.706}{4}$.

Figures 4(a) and (b) show the frequency deviations of the microgrid system for the above cases. It is clear that the cyber-physical microgrid system is asymptotically stable because of the continuous

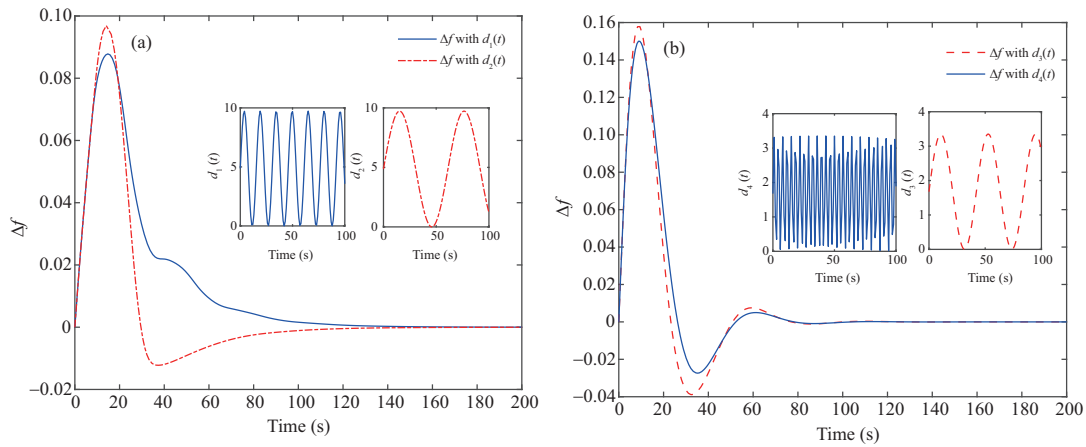


Figure 4 (Color online) Frequency deviation of the microgrid system with $d(t) \in [0, 9.730]$ (a) and $d(t) \in [0, 6.706]$ (b).

convergence of the frequency derivative.

6 Conclusion

The problem of stability analysis for the cyber-physical microgrid system with interval time-varying delay is addressed. The following findings are obtained. (1) By introducing free variables, the proposed quadratic convex framework achieves a higher degree of freedom, thus relaxing the quadratic function negative-determination condition. (2) Based on the suitable LKF and the novel quadratic convex conditions, the stability analysis criteria for the cyber-physical LFC microgrids are indeed less conservative. (3) The obtained delay margin can guide the designing and tuning of the MGCC of the LFC scheme to achieve a stable operation. In the future work, we plan to extend the quadratic convex framework with the bigger freedom developed in this study to address the stability problem and design a resilient distributed control strategy of the microgrid LFC system under cyberattacks.

Acknowledgements This work was supported partially by National Natural Science Foundation of China (Grant Nos. 62073269, 61873205), China Postdoctoral Science Foundation (Grant No. 2018M643661), Aeronautical Science Foundation of China (Grant No. 2020Z034053002), and Key Research & Development Project in Shaanxi Province (Grant No. 2022GY-244).

References

- Hatziaargyriou N D. Microgrids: Architectures and Control. Piscataway: Wiley-IEEE Press, 2014
- Li J, Ma G Q, Li T, et al. A Stackelberg game approach for demand response management of multi-microgrids with overlapping sales areas. *Sci China Inf Sci*, 2019, 62: 212203
- Farrokhhabadi M, Canizares C A, Simpson-Porco J W, et al. Microgrid stability definitions, analysis, and examples. *IEEE Trans Power Syst*, 2020, 35: 13–29
- Zamora R, Srivastava A K. Controls for microgrids with storage: review, challenges, and research needs. *Renew Sustain Energy Rev*, 2010, 14: 2009–2018
- Kundur P. Power System Stability and Control. Beijing: China Electric Power Press, 1994
- Kaur A, Kaushal J, Basak P. A review on microgrid central controller. *Renew Sustain Energy Rev*, 2016, 55: 338–345
- Geng H, Wang Z, Yi X, et al. Tobit Kalman filtering for fractional-order systems with stochastic nonlinearities under round-robin protocol. *Int J Robust Nonlinear Control*, 2021, 31: 2348–2370
- Geng H, Wang Z, Alsaadi F E, et al. Federated Tobit Kalman filtering fusion with dead-zone-like censoring and dynamical bias under the round-robin protocol. *IEEE Trans Signal Inf Process over Networks*, 2021, 7: 1–16
- Wang L, Wang Z, Shen B, et al. Recursive filtering with measurement fading: a multiple description coding scheme. *IEEE Trans Automat Contr*, 2021, 66: 5144–5159
- Wang L, Wang Z, Wei G, et al. Observer-based consensus control for discrete-time multiagent systems with coding-decoding communication protocol. *IEEE Trans Cybern*, 2019, 49: 4335–4345
- Liu S, Wang Z, Wang L, et al. Recursive set-membership state estimation over a FlexRay network. *IEEE Trans Syst Man Cybern Syst*, 2022, 52: 3591–3601
- Liu S, Wang Z, Wang L, et al. H_∞ pinning control of complex dynamical networks under dynamic quantization effects: a coupled backward Riccati equation approach. *IEEE Trans Cybern*, 2022, 52: 7377–7387
- Yang F, He J, Wang D. New stability criteria of delayed load frequency control systems via infinite-series-based inequality. *IEEE Trans Ind Inf*, 2018, 14: 231–240
- Fu Y, Zhang H Y, Mi Y, et al. Control strategy of DFIG in hybrid micro-grid using sliding mode frequency controller and observer. *IET Gener Transm Distrib*, 2018, 12: 2662–2669
- Yang F, He J, Wang J, et al. Auxiliary-function-based double integral inequality approach to stability analysis of load frequency control systems with interval time-varying delay. *IET Control Theor Appl*, 2018, 12: 601–612

- 16 Yang F, He J, Pan Q. Further improvement on delay-dependent load frequency control of power systems via truncated B-L inequality. *IEEE Trans Power Syst*, 2018, 33: 5062–5071
- 17 Gündüz H, Sönmez Ş, Ayasun S. Comprehensive gain and phase margins based stability analysis of micro-grid frequency control system with constant communication time delays. *IET Gener Transm Distrib*, 2017, 11: 719–729
- 18 Mary T J, Rangarajan P. Delay-dependent stability analysis of microgrid with constant and time-varying communication delays. *Electric Power Components Syst*, 2016, 44: 1441–1452
- 19 Vijeswaran D, Manikandan V. Stability analysis of cyber-physical micro grid load frequency control system with time-varying delay and non-linear load perturbations. *Comput Modeling Eng Sci*, 2019, 121: 801–813
- 20 Ramakrishnan K, Vijeswaran D, Manikandan V. Stability analysis of networked micro-grid load frequency control system. *J Anal*, 2019, 27: 567–581
- 21 Hua C, Wang Y, Wu S. Stability analysis of micro-grid frequency control system with two additive time-varying delay. *J Franklin Inst*, 2020, 357: 4949–4963
- 22 He Y, Wang Q G, Lin C, et al. Augmented Lyapunov functional and delay-dependent stability criteria for neutral systems. *Int J Robust Nonlinear Control*, 2010, 15: 923–933
- 23 He J, Liang Y, Yang F. Robust control for a class of cyber-physical systems with multi-uncertainties. *Int J Syst Sci*, 2021, 52: 505–524
- 24 Liu Z W, Zhang H G, Sun Q Y. Static output feedback stabilization for systems with time-varying delay based on a matrix transformation method. *Sci China Inf Sci*, 2015, 58: 012201
- 25 He J, Liang Y, Yang F, et al. New H_∞ state estimation criteria of delayed static neural networks via the Lyapunov-Krasovskii functional with negative definite terms. *Neural Networks*, 2020, 123: 236–247
- 26 Lee T H, Park J H. A novel Lyapunov functional for stability of time-varying delay systems via matrix-refined-function. *Automatica*, 2017, 80: 239–242
- 27 Gu K. An integral inequality in the stability problem of time-delay systems. In: *Proceedings of the 39th IEEE Conference on Decision and Control*, 2010. 2805–2810
- 28 Seuret A, Gouaisbaut F. Wirtinger-based integral inequality: application to time-delay systems. *Automatica*, 2013, 49: 2860–2866
- 29 Park P G, Lee W I, Lee S Y. Auxiliary function-based integral inequalities for quadratic functions and their applications to time-delay systems. *J Franklin Inst*, 2015, 352: 1378–1396
- 30 Zeng H B, He Y, Wu M, et al. New results on stability analysis for systems with discrete distributed delay. *Automatica*, 2015, 60: 189–192
- 31 Seuret A, Gouaisbaut F. Stability of linear systems with time-varying delays using Bessel-Legendre inequalities. *IEEE Trans Automat Contr*, 2017, 63: 225–232
- 32 Jiang L, Yao W, Wu Q H, et al. Delay-dependent stability for load frequency control with constant and time-varying delays. *IEEE Trans Power Syst*, 2012, 27: 932–941
- 33 Hua C, Wang Y. Delay-dependent stability for load frequency control system via linear operator inequality. *IEEE Trans Cybern*, 2022, 52: 6984–6992
- 34 Zhang X, Han Q. New stability criterion using a matrix-based quadratic convex approach and some novel integral inequalities. *IET Control Theor Appl*, 2014, 8: 1054–1061
- 35 Yang F, Zhang H. Delay dependent stability conditions of static recurrent neural networks: a non-linear convex combination method. *IET Control Theor Appl*, 2014, 8: 1396–1404
- 36 Kim J H. Further improvement of Jensen inequality and application to stability of time-delayed systems. *Automatica*, 2016, 64: 121–125
- 37 Yang F, He J, Kang P, et al. Delay range-and-rate dependent stability criteria for systems with interval time-varying delay via a quasi-quadratic convex framework. *Int J Robust Nonlinear Control*, 2019, 29: 2494–2509
- 38 Chen J, Park J H, Xu S. Stability analysis of systems with time-varying delay: a quadratic-partitioning method. *IET Control Theor Appl*, 2019, 13: 3184–3189
- 39 Zhang C K, Long F, He Y, et al. A relaxed quadratic function negative-determination lemma and its application to time-delay systems. *Automatica*, 2020, 113: 108764
- 40 Zeng H B, Lin H C, He Y, et al. Hierarchical stability conditions for time-varying delay systems via an extended reciprocally convex quadratic inequality. *J Franklin Inst*, 2020, 357: 9930–9941